ÇOMÜ Zir. Fak. Derg. (COMU J. Agric. Fac.)
2020: 8 (2): 475–489
ISSN: 2147–8384 / e-ISSN: 2564–6826
doi: 10.33202/comuagri.754784

Araştırma Makalesi/Research Article

Hyperspectral Analysis of Grapevine Water Stress

Emre Özelkan[1*] Muhittin Karaman[2] Serkan Candar[3] Ertunga Cem Özelkan[4] Cankut Örmeci[5]

[1]Çanakkale Onsekiz Mart University, Faculty of Architecture & Design, Department of Urban and Regional Planning, 17020 Çanakkale / Turkey
[2]Istanbul Technical University, Faculty of Mines, Geology Engineering Department, 34469 İstanbul/Turkey
[3]Tekirdağ Viticultural Research Station, 59100 Tekirdag/Turkey
[4]The University of North Carolina at Charlotte, Systems Engineering & Engineering Management, 9201 University City Boulevard, Charlotte/ USA
[5]Istanbul Technical University, Faculty of Civil Engineering, Department of Geomatics Engineering, 34469 Maslak, Istanbul/Turkey
*Corresponding author: emreozelkan@comu.edu.tr

Received: 18.06.2020 Accepted: 14.09.2020

Abstract

Viticulture is very sensitive to water stress, which is critical and influenced by all environmental factors, relating to the crop quality and productivity of vineyards. In this study, water stress was examined in veraison and harvest stages for nine different species with spectroradiometric measurements. Leaf water potential (LWP) values from field measurements and original spectra-based (OSB) and continuum removed spectra-based (CRSB) curves were analyzed with correlation and regression analysis to find the highest related wavelengths. The analysis was done for both specific dates of field measurements (i.e. 08.08.2012 and 06.09.2012) and also in aggregate i.e. all measured data. The specific date wavelength-based analysis revealed the “red edge region” as a major water stress indicator. The highest correlated wavelength was found to be 684 nm of CRSB curves with R=0.988. For the aggregate wavelength-based water stress analysis, the “violet and green regions” were identified as the best indicators. The highest correlated wavelength was found to be 410 nm of OSB curves with R=0.820. Furthermore, the Analysis of Variance (ANOVA) testing indicates that the results are significant at relatively high confidence levels. The spectral-based method performed in this study provides fast, flexible, and non-destructive water stress measurements of grapevines when compared to classical methods.
Key Words: Grapevine, Water Stress, Hyperspectral Remote Sensing

Asma Su Stresinin Hiperspektral Analizi

Öz

Bağcılık, ürün kalitesi ve üzüm bağlarının verimliliği ile ilgili tüm çevresel faktörlerden etkilenen ve hayati bir etken olan su stresine son derece duyarlıdır. Bu çalışmada, dokuz farklı asma türü için ben düşme ve hasat dönemlerindeki asma su stresi spektroradyometrik ölçümlerle incelenmiştir. Arazi ölçümleri ile elde edilen yaprak su potansiyeli (LWP) değerleri ile en ilişkili dalga boylarını bulmak için orijinal spektrum temelli (OSB) ve sürekliliği kaldırılmış spektrum temelli (CRSB) eğriler korelasyon ve regresyon analizi ile analiz edilmiştir. Analizler hem ölçüm tarihleri için ayrı ayrı değerlendirmeler ile (yani 08.08.2012 ve 06.09.2012) hem de tüm ölçüm verileri için toplam tek bir veri seti olacak şekilde iki farklı yaklaşım ile gerçekleştirilmiştir. Ölçümlerin ayrı ayrı analizi, “kırmızı kenar bölgesini” önemli bir su stres göstergesi olarak ortaya çıkarmıştır. En yüksek korelasyonun R = 0.988 değeri ile CRSB eğrisinin 684 nm dalga boyu olduğu belirlenmiştir. Tüm ölçümlerin bir arada değerlendirildiği su stresi analizi için “mor ve yeşil bölgeleri” en iyi göstergeler olarak tespit edilmiştir. En yüksek korelasyonun R = 0.820 değeri ile OSB eğrisinin 410 nm dalga boyu olduğu belirlenmiştir. Ayrıca, Analysis of Variance (ANOVA) testinin sonuçları bu çalışmada elde edilen bulguların yüksek güven seviyelerinde anlamlı olduğunu göstermektedir. Bu çalışmada gerçekleştirilen spektral tabanlı yöntem, üzüm bağlarının / asma su stresi ölçmelerini klasik yöntemlere kıyasla hızlı, esnek ve tahribatsız bir şekilde sağlamaktadır.
Anahtar Kelimeler: Asma, Su Stresi, Hiperspektral Uzaktan Algılama

ÇOMÜ Zir. Fak. Derg. (COMU J. Agric. Fac.)
2020: 8 (2): 475–489
ISSN: 2147–8384 / e-ISSN: 2564–6826
doi: 10.33202/comuagri.754784

Introduction:

Plant water stress determination and measurement is vital and necessary for many forestry, agricultural, land rehabilitation and conservation applications (Govender et al., 2009; Demirel et al., 2014; Demirel et al., 2018; Camoglu et al., 2018; Camoglu et al., 2019a). Grapevine physiology (Naor et al., 1994; Williams and Araujo, 2002; De Bei et al., 2011), vegetative and reproductive growth (Schultz and Matthews, 1993) and yield has been highly correlated with water stress (Greenspan et al., 1996; Williams and Araujo, 2002). Grapevine productivity and quality are highly related to water stress (Kennedy et al. 2002; Cifre et al., 2005; Rodríguez-Pérez et al., 2007; De Bei et al., 2011). Leaf water potential (LWP) is typically used as an indicator of water stress, which provides information about soil type, soil moisture, salinity, available water, environmental conditions, agronomic practices, crop growth and climate as an integrated system. (Turner, 1981; Williams and Araujo, 2002; Eitel et al., 2006; Kakani et al., 2007; Gutierrez et al., 2010).

Pressure chamber technique, which is a frequently used destructive LWP measurement method, provides a simple, reliable, rapid, economical and portable LWP measurement (Scholander et al., 1965; Ritchie and Hinckley, 1975; Eitel et al., 2006; Govender et al., 2009; Gutierrez et al., 2010; De Bei et al., 2011; Camoglu et al., 2019a). This technique can be used to identify correlations between the water stress and the grapevine physiology (Williams and Araujo 2002; Rodríguez-Pérez et al., 2007).

Remote sensing is frequently used in agricultural monitoring (Ozelkan et al., 2016; Gürsoy and Atun 2018) and provides successful results especially in plant condition analysis studies (İnce et al. 2014; Ozelkan et al., 2015; Gürsoy and Atun 2019). Remote sensing technologies benefit from spectral reflectance data to determine plant water stress (Sims and Gamon, 2002; Stimson et al., 2005; Eitel et al., 2006; Fitzgerald et al., 2006; Govender et al., 2009; Demirel et al., 2014; Camoglu et al., 2018; Camoglu et al., 2019b). Compared to the pressure chamber technique, remote sensing techniques provide a means for a more reliable, instant, simple and nondestructive water status measurement (Hunt et al. 1989; Rodríguez-Pérez et al., 2007).

It has been shown in the literature that several wavelengths (760 nm, 970 nm, 1190 nm, 1240 nm, 1400 nm, 1450 nm, 1900 nm, 1940 nm, 2700 nm, and 2950 nm) are reactive to water absorption (Tucker, 1980; Peñuelas et al., 1993; Gao, 1996; Ceccato et al., 2001; Stimson et al., 2005; Eitel et al., 2006; Kakani et al., 2007; Rodríguez-Pérez et al., 2007; Gutierrez et al., 2010). The effect of background materials (such as soil) and atmospheric absorptions on the water absorption bands may cause sensing problems. Continuum removal analysis (CRA) is used to overcome this problem (Kokaly and Clark 1999; Rodríguez-Pérez et al., 2007). CRA gives opportunity to isolate the relevant absorption features, therefore the coefficients of determination increase and more sensitive absorption features can be identified (Kokaly and Clark 1999; Rodríguez-Pérez et al., 2007).

The purpose of this study is to introduce a hyperspectral remote sensing-based technique for water stress analysis of grapevines. To illustrate the proposed application to grapevine, leaves from nine grape species were examined by comparing mid-day LWP values and spectral reflectance measurements. LWP values were associated with both original spectra-based (OSB) and CR spectra-based (CRSB) curves and analyzed with correlation and regression analysis to find the highest related wavelengths.

Materials and Methods:

Study Area

Tekirdag is in the Eastern Thrace region of Turkey, which has a very old and rooted viticulture tradition (Durgut and Arın, 2005). The LWP and spectroradiometric measurements were performed in the national collection vineyard of Tekirdag Viticultural Research Station, which is in the boundaries of the following coordinates: northwest 40.973562°N - 27.461911°W and southeast: 40.969184°N - 27.477504°W (Figure 1). The region is under the effect of Marmara climate that is a transition climate between the Continental, the Black Sea and the Mediterranean climates, where the summers are not as rainy as the Black Sea climate and not as dry as the Continental climate, and the winters are not as warm as the Mediterranean climate and not as cold as the Continental Climate (Sensoy et al., 2008). Long year's monthly average temperature is 14°C and long year's annual total precipitation is 585 mm. The rainiest period is December with 82.8 mm, and the driest period is August with 12.5 mm

ÇOMÜ Zir. Fak. Derg. (COMU J. Agric. Fac.)
2020: 8 (2): 475–489
ISSN: 2147–8384 / e-ISSN: 2564–6826
doi: 10.33202/comuagri.754784

precipitation. The July and August are hottest periods with 24ºC, and the coldest is January with 5ºC.The climate conditions of the study area enable the growth of many grape species, which is more than 1200 according to the Tekirdag Viticultural Research Station actual report.

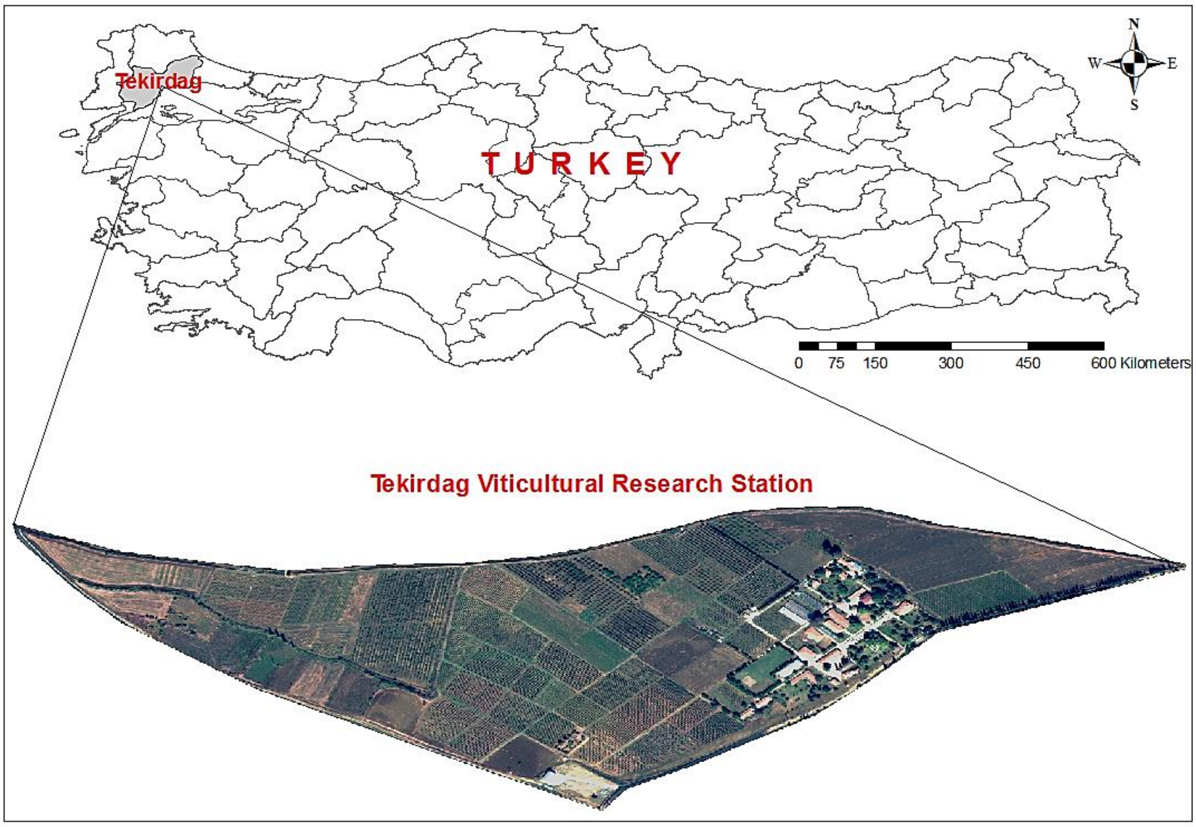

Figure 1. The study area.

LWP Measurement Method

LWP measurements were performed using the “Model 3115-Portable Plant Water Status Console- Scholander Pressure Chamber”. Note that the LWP measurements should be performed fast and carefully in two steps. First, a fully developed healthy and sun-exposed leaf is determined, which reflects the phenological era. The leaf is cut as fast as possible from the end of the petiole and placed into the pressure vessel to prevent changes from dehydration and evaporation and to get accurate results (Turner, 1988; Smith and Prichard, 2003; Eitel et al., 2006; Govender et al., 2009). Second, the vessel is pressurized until the first exudation of sap from the cut surface of petiole. This pressure is where the negative of the atmospheric pressure is equal to the plant’s hydrostatic pressure and therefore it is equal to LWP (Turner, 1988; Smith and Prichard, 2003; Eitel et al., 2006; Govender et al., 2009). LWP measurements were performed just after spectroradiometric measurements for nine grape species.

The LWP results including temporal differences, average and standard deviation values of 9 species are summarized in Table 1. The LWP and spectral reflectance measurements were performed on 08.08.2012 (1st measurement - M1: veraison stage) and on 06.09.2012 (2nd measurement - M2: harvest stage).

According to phenological era, the average water stress of the M2 is higher than M1. A water stress increase was observed in the Alphonse, Atasarisi, Cinsaut, Razaki, Semilion, Tekirdag Cekirdeksizi and Yapincak, and a decrease was observed in Gamay and Merlot. The average water stress values were -1.56 MPa and -1.68 MPa on 08.08.2012 and 06.09.2012, respectively. The average difference of water stress between two phenological stages is 0.13 MPa. The standard deviations of

ÇOMÜ Zir. Fak. Derg. (COMU J. Agric. Fac.)
2020: 8 (2): 475–489
ISSN: 2147–8384 / e-ISSN: 2564–6826
doi: 10.33202/comuagri.754784

M1 and M2 are 0.05 Mpa and 0.17 Mpa, respectively. The standard deviation of M2 values is higher than the first one, because the species differ, in shape during or after the harvest stage.

Table 1. The water stress results (Ψ_{leaf}(-MPa): mid-day LWP leaf in negative megapascal).

Species	08.08.2012 $\Psi_{leaf(-MPa)}$	06.09.2012 $\Psi_{leaf(-MPa)}$	Difference $\Psi_{leaf(-MPa)}$
Alphonse Lavallée	-1.55	-1.85	0.30
Atasarisi	-1.52	-1.66	0.14
Cinsaut	-1.60	-1.65	0.05
Gamay	-1.52	-1.35	-0.17
Merlot	-1.65	-1.58	-0.07
Razaki	-1.60	-1.86	0.26
Semillion	-1.50	-1.62	0.12
Tekirdag Cekirdeksizi	-1.52	-1.90	0.38
Yapincak	-1.50	-1.64	0.14
Average	-1.55	-1.68	0.13
Standard Deviation	0.05	0.17	0.17

The temporal change of water stress was examined due to meteorological and phenological changes in this section. It is well-known that events like slowdowns in development and photosynthesis activity, and rises at water stress depend on the decrease in soil moisture and the harvest phenological stage (Carbonneau, 1998; Bertamini and Nedunchezhian, 2003; Deloire et al, 2004; Ozelkan et al. 2015). Although such events trigger the increase in water stress, the difference of average of water stress between two phenological stages is not much in our case, which can be explained based on the meteorological data. Between the two measurement dates, there had been only 6.2 mm precipitation. Considering the evapotranspiration in summer, the 6.2 mm precipitation value is not sufficient to make the soil moist. Accordingly, the water stress increases until the rainy season.

Other meteorological parameters of the measurements' eras are given in Table 2. All physiological activities of plants, particularly photosynthesis, can be continued at optimum level between 25-30°C (Ferrini et al., 1995; Uzun, 2004; Greer and Weedon 2012). Higher temperatures trigger the water stress with the increase in the amount of water into the air by transpiration. The average temperature of M1 and M2 (14:00-15:00) are 32.46°C and 27.56°C, respectively. The average solar radiation of M1 and M2 (14:00-15:00) are 3413.15 $\mu mol.s^{-1}m^{-2}$ and 2994.77 $\mu mol.s^{-1}m^{-2}$ respectively. Based on these findings, we can conclude that M1 conditions would lead to higher water stress. The average UV of M1 and M2 (14:00-15:00) are 6.6 and 5.17, which are in moderate to high levels according to the UV index (TSMS, 2013; ARPANSA, 2013; CCOHS, 2013). Again, based on UV values, first day measurements should be more stressful than the second. Decrease in relative humidity (RH), in other words, the increase of vapor pressure difference between plant and air expedites water lose due to transpiration and again, the plant enters to a state of water stress (Eamus and Shanahan, 2002). The average RH of M1 and M2 (14:00-15:00) are 48.14% and 62.23% respectively, thus first day measurements should be more stressful than the second based on the RH as well. Increase in wind speed causes to trigger the increase in transpiration that again causes water stress (Lambers et al., 2008). The average wind speed of M1 and M2 (14:00-15:00) are 14 $km.h^{-1}$ and 10.92 $km.h^{-1}$ respectively, thus, first day measurements should be more stressful than the second depend on the wind speed.

Table 2. 10-minute frequency average meteorological parameters in the measurement time intervals.

Measurement Dates	Atmospheric Pressure (mb)	UV	2 m Air Temperature (°C)	Relative Humidity (%)	Wind Direction	Wind Speed ($km.h^{-1}$)	Solar Radiation Intensity ($\mu mol.s^{-1}m^{-2}$)
08.08.2012	1012.79	6.6	32.46	48.14	7	14.04	3413.15
06.09.2012	1011.29	5.1	27.56	62.23	7.08	10.92	2994.77

As discussed above, according to analysis of available meteorological data, the water stress average of the M1 is expected to be higher. On the other hand, according to phenological era, the water stress average of the M2 is expected to be higher. It seems overall, the phenological conditions have slightly stronger influence than the meteorological conditions, thus the water stress average of the M2 values turned out to be slightly higher than M1. The M1 and M2 phenological stages, conditions, information and photos of the corresponding species are presented in Table 3 and Figure 2. In M1, none of the species were in harvest phase, and even fruits of some species did not fully reach maturity. In M2, five of the species (Alphonse Lavallée, Atasarisi, Gamay, Merlot, Tekirdag Cekirdeksizi) just passed the harvest phase, four of them (Cinsaut, Razaki, Semilion, Yapincak) were very close to the harvest phase.

Table 3. The 2012 phenological stages' dates of studied species.

Species	Bud Burst	Flowering	Veraison	Harvest
Alphonse Lavallée	06.04.2012	28.05.2012	23.07.2012	27.08.2012
Atasarisi	05.04.2012	02.06.2012	25.07.2012	25.08.2012
Cinsaut	05.04.2012	30.05.2012	26.07.2012	07.09.2012
Gamay	04.04.2012	28.05.2012	20.07.2012	16.08.2012
Merlot	04.04.2012	28.05.2012	23.07.2012	04.09.2012
Razaki	06.04.2012	30.05.2012	03.08.2012	12.09.2012
Semillion	05.04.2012	28.05.2012	03.08.2012	11.09.2012
Tekirdag Cekirdeksizi	04.04.2012	29.05.2012	30.07.2012	24.08.2012
Yapincak	02.04.2012	28.05.2012	03.08.2012	11.09.2012

ÇOMÜ Zir. Fak. Derg. (COMU J. Agric. Fac.)
2020: 8 (2): 475–489
ISSN: 2147–8384 / e-ISSN: 2564–6826
doi: 10.33202/comuagri.754784

Figure 2. M1 (left) and M2 (right) phenological conditions of the corresponding species.

Spectral Reflectance Measurement Method

ASD Handheld Spectroradiometer operating in a spectral range of [375-1075] nm was used to get the spectral reflectance of leaves. For each spectral application, the distances of dark current correction, optimization, white reference and measurement were set to be same (10 cm) above the vine leaf from a nadir orientation. The measurements were performed using a one-degree lens. The field of view was 1°, covering a circular area of 0.1745 cm in diameter and the swath area of 0.0239 cm^2. At least 10 iterations were made for spectral reflectance measurement of each species, then the anomaly curves were eliminated and the mean of 10 spectral curves was averaged to find the final spectral curve of each grape species. Spectroradiometric measurements were performed just before LWP measurements for the nine species. Finally, the values between [400-1000] nm were chosen in this study due to the high noise outside this interval.

CR normalizes reflectance spectra in order to allow comparison of individual absorption features from a common baseline (Clark, 1999; Kokaly and Clark 1999; Kokaly, 2001; Mutanga, 2003; Rodríguez-Pérez et al., 2007). Convex hull fitted over the top of a spectrum is called the continuum. The CR reflectance, Rcr(λ) of each wavelength is generated by dividing the original reflectance value Ro(λ) to the reflectance value of the convex hull (continuum line) Rcl(λ) of the corresponding wavelength (Equation [1]). Based on this relationship, if the spectrum and continuum line are matching, the Rcr(λ) value will be 1, on the other hand, if there is absorption, the Rcr(λ) value would decrease. (Schmidt and Skidmore, 2003; Mutanga, 2003; Rodríguez-Pérez et al., 2007).

$$Rcr(\lambda) = Ro(\lambda)/Rcl(\lambda) \quad [1]$$

ÇOMÜ Zir. Fak. Derg. (COMU J. Agric. Fac.)
2020: 8 (2): 475–489
ISSN: 2147–8384 / e-ISSN: 2564–6826
doi: 10.33202/comuagri.754784

OSB and CRSB curves corresponding to the M1 and M2 spectral measurement and multi temporal difference spectrum results are shown in Figure 3. In the original spectral curves, the high differences are shown in mostly in the red edge and there are also variations at the visible region. In contrast, the high differences are shown at the visible regions in the CR spectral curves. Multi temporal difference spectra were used to define the phenological variations of water stress in further sections. In multi temporal difference spectra, green and red edge regions seem to contain more variations between species.

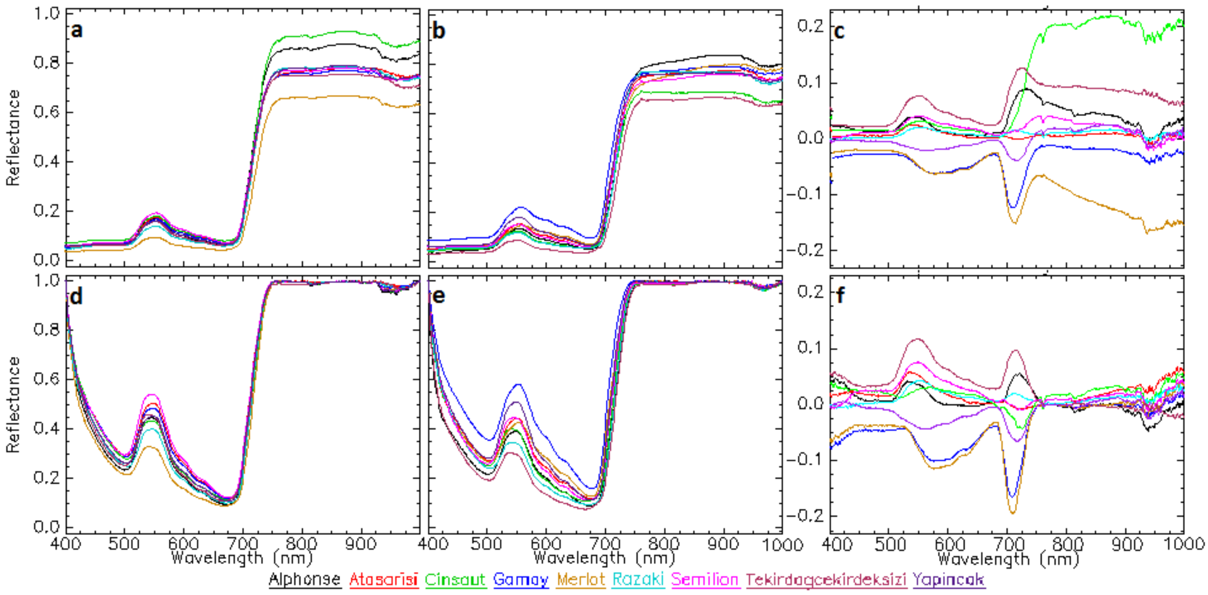

Figure 3. a: M1 OSB-Curves, b: M2 OSB-Curves, c: OSB difference spectrum, d: M1 CRSB-Curves, e: M2 CRSB-Curves, f: CRSB difference spectrum.

Data Analysis

The relations between the water stress (LWP) and hyperspectral values were analyzed with correlation and regression analyses. In the result section, Pearson correlation coefficient (R) and coefficient of determination (R^2) values of the findings were showed individually for each wavelength. Simple linear regression models were developed to verify trends. In addition, the significance of results was analyzed using Analysis of Variance (ANOVA), and Root Mean Square Error (RMSE). The following section will present the major findings and recommendations based on the analysis.

Results and Discussion:

Specific Dates Analysis

In this part of the study, the analysis of specific dates (08.08.2012 & 06.09.2012) and optimum intersection specific dates will be presented. OSB and CRSB from of 9 spectra were individually correlated with 9 water stress values to find the most sensitive wavelengths for 08.08.2012 and 06.09.2012, respectively.

Analysis of the relation between water stress and OSB & CRSB-Curves using specific dates measurement

Study with OSB-Curves: Correlation coefficients between water stress and original spectral reflectance values for the 9 grape species are shown in Figure 4 for each wavelength for M1 and M2 measurements. [400-730] nm interval of each veraison and harvest stages were found to be highly correlated with water stress. M1 was found to be less correlated with [400-730] nm compared to M2. The M2 water stress values influence the electromagnetic spectrum much more than M1 especially in [400-510] nm and [630-680] nm, where correlation is expected with chlorophyll content and plant stress (Chappelle et al, 1992; Carter and Miller, 1994; Zarco-Tejada et al., 2000; Govender et al., 2009). The reason why M2 is much more correlated with spectra can be explained as follows: The water stress values and standard deviation value of M1 were smaller than the M2 values. Based on the distinctive phenological stage differences, M2 was found to be more sensitive to spectra.

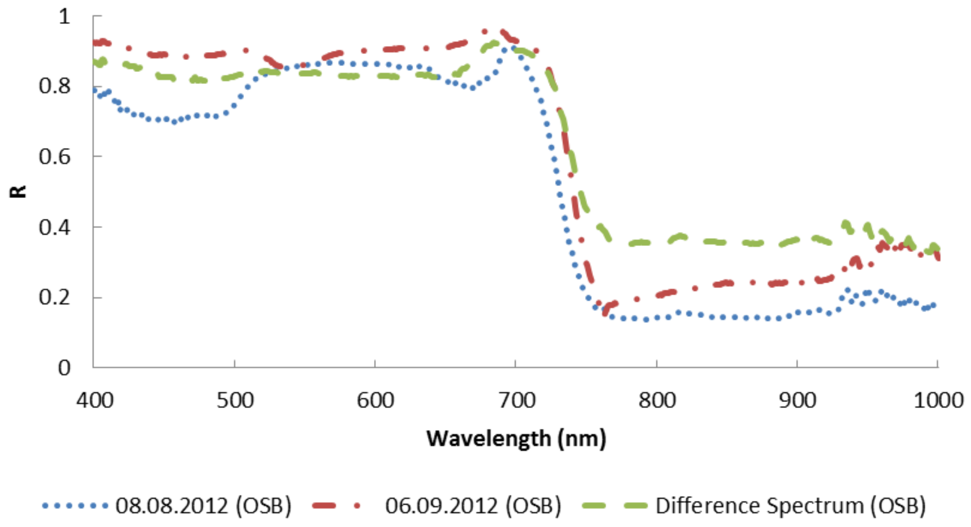

Figure 4. Correlations between water stress and OSB-Curves' values for M1 and M2, and correlation between temporal difference of Ψ_{leaf}(-MPa) and temporal difference of OSB-Curves.

In the M1 analysis, [510-662] nm and [672-713] nm intervals were found to be R≥0.8 correlated with water stress. The highest correlation was found at 695 nm with R=0.914 (R^2=0.8357). In the M2 analysis, [400-726] nm interval was found to be R≥0.8 correlated with water stress. The highest correlation was found at 686 nm with R=0.972 (R^2=0.9453). 695 and 686 nm wavelengths are in the red edge region. The temporal difference values of water stress (Table 1) and OSB-Curves Figure 3 were computed to find the correlated wavelengths that are sensitive to temporal change of water stress. Generally, ~560 nm and ~715 nm regions were found to be more sensitive to differentiations in temporal original spectra. In the interval of [400-726] nm, R≥0.8 was found and the highest correlation was found at 684 nm with R=0,924 (R^2=0,853). Figure 5 shows the individual linear regression models and corresponding R^2 values for 684, 686 and 695 nm wavelengths. As seen from the figure and based on the corresponding analysis of variance (presented in section 4.3), the linear models provide a good and statistically significant fit (with significance probabilities close to zero and >99 % confidence level).

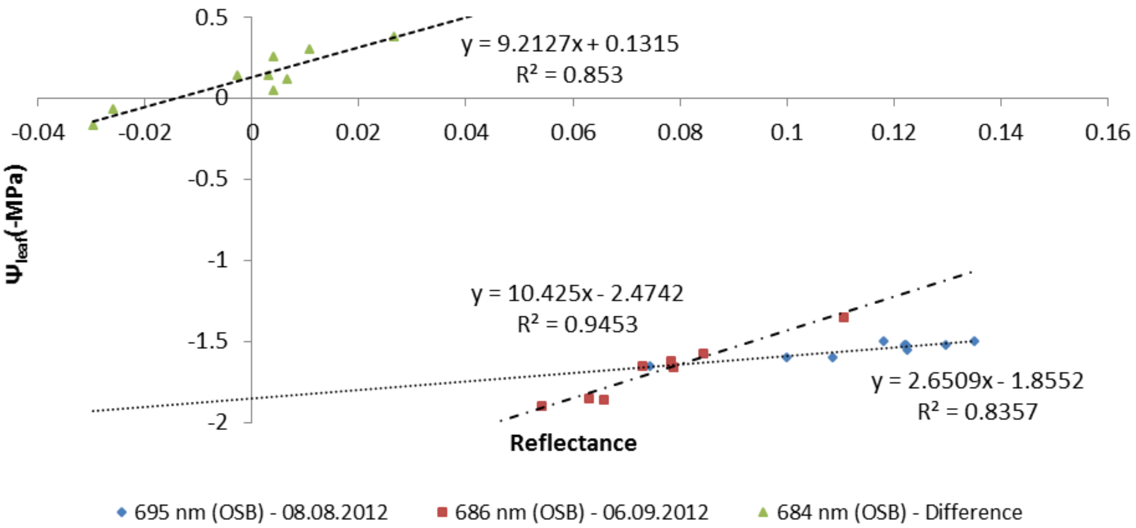

Figure 5. The relation between M1 Ψ_{leaf}(-MPa) values and 695 nm of OSB-Curves, M2 Ψ_{leaf}(-MPa) values and 686 nm of OSB-Curves and temporal difference of Ψ_{leaf}(-MPa) and temporal difference of 684 nm of OSB-Curves.

ÇOMÜ Zir. Fak. Derg. (COMU J. Agric. Fac.)
2020: 8 (2): 475–489
ISSN: 2147–8384 / e-ISSN: 2564–6826
doi: 10.33202/comuagri.754784

<u>*Study with CRSB-Curves:*</u> Correlations between water stress and CR spectra values are shown in Figure 6 for each wavelength for M1 and M2. Compared to the OSB-curves analysis, the correlation between M1 and CRSB-curves was found to be lower.

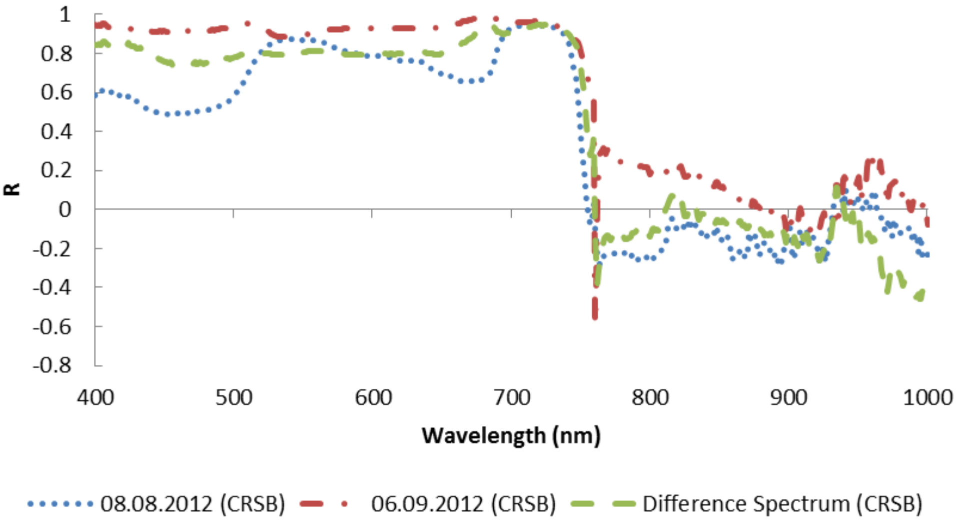

Figure 6. Correlations between water stress and CRSB-Curves for M1 and M2, and correlation between temporal difference of Ψ_{leaf}(-MPa) and temporal difference of CRSB-Curves.

In the M1 analysis, [519-587] nm and [690-742] nm intervals were found to be R≥0.8 correlated with water stress. The highest correlation was found at 723 nm with R=0.942 (R^2=0.8869). In the M2 analysis, [400-754] nm interval was found to be R≥0.8 correlated with water stress over. The highest correlation was found at 684 nm with R=0.988 (R^2=0.9767). 723 and 684 nm wavelengths are in the red edge region as it was found in the original spectra analysis.

Similar analysis of the temporal differences of water stress (Table 1) and CRSB-Curves (Figure 3) showed that ~560 nm and ~710 nm regions are more sensitive to differentiations in multi-temporal original spectra. In the intervals of [402-435], [512-524], [545-572], [628-642] and [653-748] nm, the correlation was found as R≥0.8 and the highest correlation was found at 724 nm with R=0.945 (R^2=0.8931). Figure 7 shows the individual linear regression models and corresponding R^2 values for 684, 723 and 724 nm wavelengths. Again, the figure and the analysis of variance (presented in section 4.3) confirm that the linear models are fairly adequate in this case with high statistical significance.

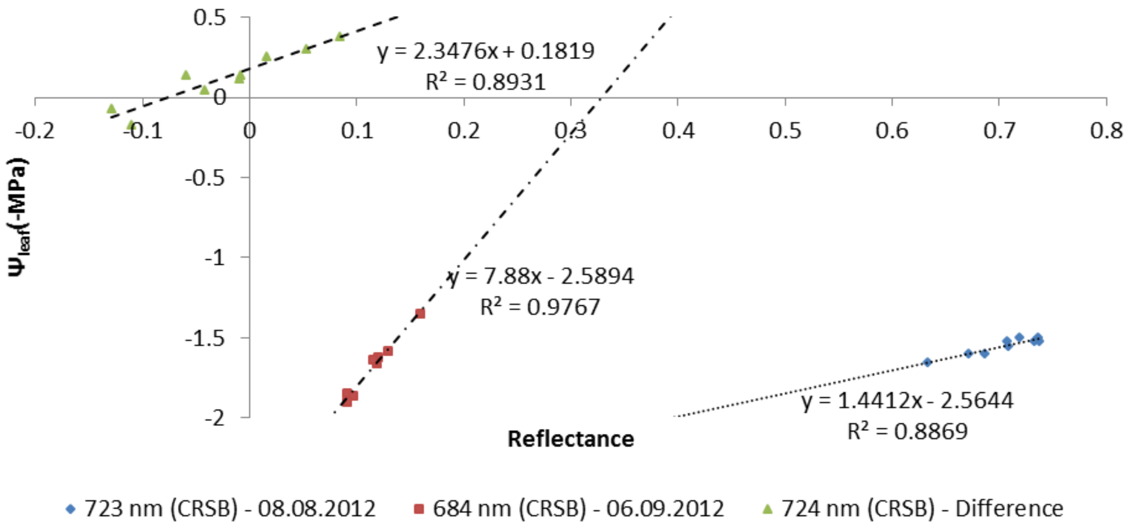

Figure 7. The relation between M1, M2, temporal difference Ψ_{leaf}(-MPa) values and 723 nm, 684 nm, 724 nm of CRSB-Curves respectively.

ÇOMÜ Zir. Fak. Derg. (COMU J. Agric. Fac.)
2020: 8 (2): 475–489
ISSN: 2147–8384 / e-ISSN: 2564–6826
doi: 10.33202/comuagri.754784

Aggregate Analysis

So far, the analysis was conducted for different dates of the veraison and harvest stages (i.e. specific dates) separately (08.08.2012 and 06.09.2012). In this section, a consolidated analysis (i.e. aggregate analysis) is presented for the total data (9+9=18 spectra and water stress data corresponding to 08.08.2012 and 06.09.2012).

Analysis of the Relation between Water Stress and OSB&CR Curves using Aggregate Data

Correlations between total water stress values and original and CR spectra values are shown in Figure 8 for each wavelength. OSB curves and water stress correlation distribution were found more homogeneous than the correlation of CRSB and water stress. In the previous sections, it was indicated that the CRSB curves detect the absorption feature and main differentiation regions of spectra and thus this causes heterogeneity in the correlation distribution. ~760 nm, ~820 nm and ~930 nm regions were identified as correlation anomalies with low R values in current study as seen in Figure 8. These results seem to comply with the literature as "~690 nm = O2, ~720 nm = H20, ~760 nm = O2, ~820 nm = H2O, ~930 nm = H2O" were indicated as molecular absorption and sensitivity regions (Borengasser et al., 2004; Mohan, 2008).

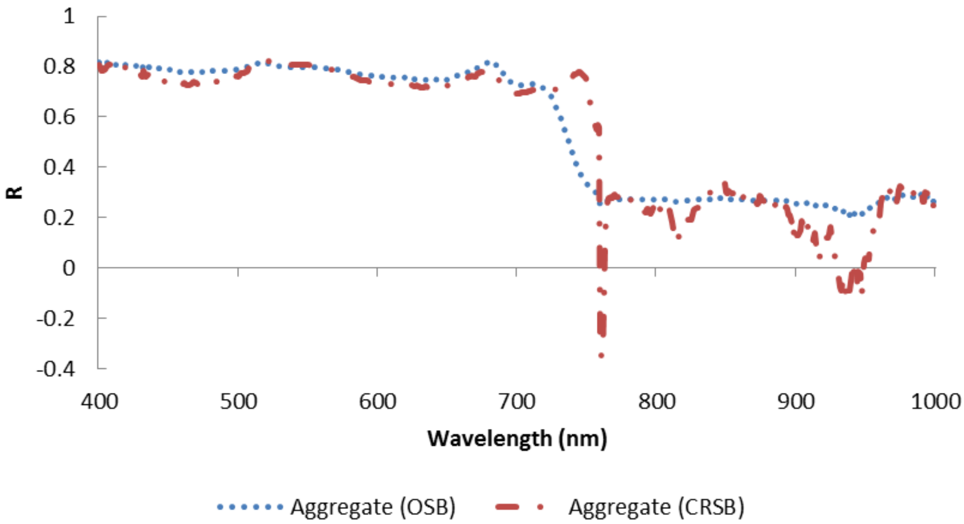

Figure 8. Correlations between aggregate water stress values of grape species and OSB and CRSB-Curves.

Study with OSB Curves: In the original spectra analysis, [400-432], [507-529] and [673-687] nm intervals were found to be R≥0.8 correlated with water stress. The highest correlation was found at 410 nm with R=0.820 (R^2=0.6728) (Figure 8). 410 nm is in the violet region.

Study with CRSB Curves: In the CR spectra analysis, [400-420] and [512-559] nm intervals were found to be R≥0.8 correlated with water stress. The highest correlation was found at 521 nm with R=0.820 (R^2=0.6722) (Figure 9). 521 nm is in the green region.

Figure 9 shows the individual linear regression models and corresponding R^2 values for 410 and 521 nm wavelengths, which again seem fairly adequate in this case. Next, we will elaborate on the statistical significance of these results using the Analysis of Variance (ANOVA) methodology.

ÇOMÜ Zir. Fak. Derg. (COMU J. Agric. Fac.)
2020: 8 (2): 475–489
ISSN: 2147–8384 / e-ISSN: 2564–6826
doi: 10.33202/comuagri.754784

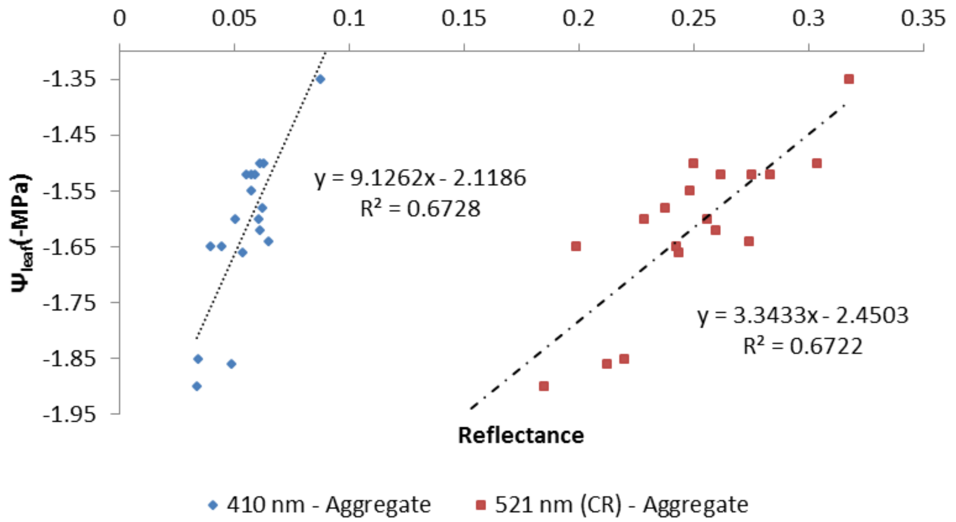

Figure 9. The relation between 410 nm of aggregate OSB and Ψ_{leaf}(-MPa) and the relation between 521 nm of aggregate CRSB and Ψ_{leaf}(-MPa).

Analysis of Variance - ANOVA

The significance of results was analyzed for each wavelength and the corresponding linear relationship using ANOVA and RMSE. The names of determined wavelengths, data used, spectra type (ST), associated formula, multiple R (M-R), coefficient of determination R^2, adjusted R^2 (A-R^2), significance F (S-F), and RMSE results are given in Table 4. The rest of the information corresponding to the ANOVA tables (such as degrees of freedom, sum of squares, and F values) was not shown here for conciseness. S-F values from the ANOVA were found to be very small that indicates very good regression relation between wavelength and water stress. For example, in the analysis between OSB 695 nm and water stress of 08.08.2012, S-F was found 0.000561 that indicates 99.9439% (=100×[1-0.000561]) confidence on the established relation. In addition, the RMSE values are smaller than 0.1 that also indicates a high accuracy of results.

Table 4. ANOVA and Root Mean Square Error (RMSE) analysis results

Wavelength	Data used	ST	Formula	M-R (R)	R^2	(A- R^2)	S-F	RMSE
695 nm	8.08.2012	OSB	y = 2.6509x - 1.8552	0.914142	0.835656	0.812178	0.000561	0.020355
686 nm	6.09.2012	OSB	y = 10.425x - 2.4742	0.972241	0.945252	0.937431	0.000011	0.037816
684 nm	Difference	OSB	y = 9.2127x + 0.1315	0.923553	0.85295	0.831943	0.000377	0.063264
723 nm	8.08.2012	CRSB	y = 1.4412x - 2.5644	0.941739	0.886873	0.870712	0.000148	0.016888
684 nm	6.09.2012	CRSB	y = 7.88x - 2.5894	0.98826	0.976657	0.973323	0.000001	0.024693
724 nm	Difference	CRSB	y = 2.3476x + 0.1819	0.945041	0.893103	0.877832	0.000121	0.053939
410 nm	Aggregate	OSB	y = 9.1262x - 2.1186	0.820218	0.672758	0.652305	0.000031	0.077603
521 nm	Aggregate	CRSB	y = 3.3433x - 2.4503	0.819854	0.67216	0.65167	0.000031	0.077673

Conclusions:

In this study, we applied a remote sensing-based spectroradiometric technique for water stress analysis of grapevines. Considering the specific dates of veraison and harvest stages first, the study results showed that the best wavelength-based indicator of LWP is in the red edge region for both OSB and CR data. Red edge, which is approximately between a minimum range of [690-740] nm and a maximum range of [670-780] nm is highly related with plant water stress) Jayaraman and Srivastava, 2002; Fitzgerald et al., 2006; Eitel et al., 2006; Blackburn, 2007; Govender et al., 2009; Liu et a., 2013). The results are in alignment with the previous studies that reported that the shape and position of red edge was found to be an indicator of chlorophyll content, biomass and hydric status of plants

(Penuelas et al., 1993; Filella and Penuelas, 1994; Liu et al., 2013) and highly correlated with water stress of grapevines (Broge and Leblanc 2001; Rodríguez-Pérez et al., 2007).

High correlations of OSB-Curves and the LWP values were found to be R= 0.914 (R^2=0.8357) at 695 nm and R=0.972 (R^2=0.9453) at 686 nm for M1 and M2 specific dates, respectively. The correlation between temporal difference spectra and LWP data was found to be most correlated with 684 nm with R=0.924 (R^2=0.853). High correlations of CRSB-Curves and the LWP values were found to be R=0.942 and R^2=0.8869 at 723 nm for M1 and R=0.988 and R^2=0.9767 at 684 nm for M2. The correlation between temporal differences spectra and LWP data was found to be most correlated with 724 nm with R= 0.945 and R^2=0.8931. In other words, if red edge reflectance increases, the water stress decreases.

When the data was analyzed as an aggregate (total data of 18 points), good correlations were found with water stress between 400-432 nm (in the violet region), 507-559 nm (in the green region) and 673-687 nm (in the end of the red and beginning of the red edge). Note that these findings are in alignment with previous research which showed correlations between chlorophyll content and plant stress (Chappelle et al, 1992; Carter and Miller, 1994; Zarco-Tejada et al., 2000; Govender et al., 2009). In other words, as an aggregate result of the current study, if violet, green and red-red edge reflectance increases, water stress decreases. An ANOVA analysis confirmed that the findings are statistically significant at over 99% confidence levels.

Consequently, the OSB and CRSB results were found to be similar in most part. According to specific date's analysis results, the water stress is highly correlated with the red edge region wavelengths. According to aggregate (total data) analysis' results, the water stress values are highly correlated with violet, green and red edge region.

Water is vitally important for all living things and lack of water causes stress. Viticulture, which is a precious agricultural activity, is excessively influenced by all environmental factors. Spectral data provides integrated information about a plant reflecting soil type, soil moisture, salinity, available water, environmental conditions, agronomic practices, crop growth and climate. In addition, hyperspectral spectroradiometric techniques supply non-destructive measurement method compared to the traditional pressure chamber's LWP. This study may be useful to monitor the water status and stress of grapevine and the other plants using remote sensing. The hyperspectral remote sensing findings may be adapted and tried in the different satellite, airborne or in-situ remote sensing sensors such as multispectral and hyperspectral and others. The findings may be used for different activities associated with plant such as agriculture and forestry. The irrigation scheduling of agricultural-viticultural activities may be organized and determined using the results and finding of this study. However, wavelengths were found and verified with water stress values, the other measurements of different parameters such as soil moisture, photosynthesis, leaf temperature and stoma conductance and others that affect plant water stress may be performed in the future studies. As compared with the classical methods, this study validates that the spectral-based methods provide faster, more flexible application, more sensitive and non-destructive water stress measurements.

Acknowledgements:

The authors thank to the Tekirdag Viticultural Research Station for enabling research and use of the pressure chamber for LWP measurements, furthermore to Istanbul Technical University, Satellite Communication and Remote Sensing Centre for their support with the spectroradiometer device used in spectral measurements.

References:

Australian Radiation Protection and Nuclear Safety Agency (ARPANSA)., 2013. Radiation Protection - Solar UV radiation and the UV Index. http://www.arpansa.gov.au/radiationprotection/factsheets/is_UVindex.cfm

Bertamini, M. and Nedunchezhian, N., 2003. Photosynthetic functioning of individual grapevine leaves (Vitis vinifera L. cv. Pinot noir) during ontogeny in the field. Vitis 42 (1), 13–17.

Blackburn, G.A., 2007. Hyperspectral remote sensing of plant pigments. Journal of Experimental Botany, 58(4), 855-867, doi: 10.1093/jxb/erl123

Broge, N.H. and Leblanc, E., 2001. Comparing prediction power and stability of broadband and hyperspectral vegetation indices for estimation of green leaf area index and canopy chlorophyll density. Remote Sensing of Environment, 76(2), 156-172, http://dx.doi.org/10.1016/S0034-4257(00)00197-8

Borengasser, M., Hungate, W.S. and Watkins, R., 2004. Hyperspetral Remote Sensing. CRC Press, 1st ed., Florida.

Canadian Centre for Occupational Health and Safety (CCOHS)., 2013. Ultraviolet Radiation. http://www.ccohs.ca/oshanswers/phys_agents/ultravioletradiation.html

Carter, G.A. and Miller, R.L., 1994. Early Detection of Plant Stress by Digital Imaging within Narrow Stress-Sensitive Wavebands. Remote Sensing of Environment, 50(3), 295-302, ttp://dx.doi.org/10.1016/0034-4257(94)90079-5

Carbonneau, A., 1998. Aspects Qualitatifs. 258-276. In: Tiercelin, JR (Ed.), Traite d'irrigation. Tec&Doc. Lavosier Ed., Paris, 1011 p.

Ceccato, P., Flasse, S., Tarantola, S., Jacquemoud, S. and Gregoire, J.M., 2001. Detection vegetation leaf water content using reflectance in the optical domain. Remote Sensing of Environment, 77(1), 22-33, http://dx.doi.org/10.1016/S0034-4257(01)00191-2

Chappelle, E.W., Kim, M.S. and McMurtrey, J.E., 1992. Ratio analysis of reflectance spectra (RARS): an algorithm for the remote estimation of the concentrations of chlorophyll a, chlorophyll b, and carotenoids in soybean leaves. Remote Sensing of Environment, 39(3), 239-247, http://dx.doi.org/10.1016/0034-4257(92)90089-3

Cifre, J., Bota, J., Escalona, J.M., Medrano, H. and Flexas, J., 2005. Physiological tools for irrigation scheduling in grapevine (Vitis vinifera L.): an open gate to improve water-use efficiency? Agriculture Ecosystems and Environment, 106(2005), 159–170, doi:10.1016/j.agee.2004.10.005

Clark, R. N., 1999. Chapter 1: Spectroscopy of Rocks and Minerals, and Principles of Spectroscopy, in Manual of Remote Sensing, Remote Sensing for the Earth Sciences, (A.N. Rencz, ed.) John Wiley and Sons, New York, 3, 3- 58

Çamoğlu, G., Demirel, K., Genc, L., 2018. Use of Infrared Thermography and Hyperspectral Data to Detect Effects of Water Stress on Pepper. Quantitative InfraRed Thermography Journal. 15(1):81-94.

Çamoğlu G., Akçal A., Demirel K., Genç L., 2019a. Su Stresinin Sofralık Domatesin Verimi ve Fizyolojik Özellikleri Üzerine Etkileri. Bursa Uludağ Üniversitesi Ziraat Fakültesi Dergisi, vol.33, pp.15-30,

Çamoğlu G., Demirel K., Genç L., 2019b. Termal Kamera ve NDVI Sensörü kullanılarak Domatesin Fizyolojik Özelliklerinin tahminlenmesi. Harran Tarım ve Gıda Bilimleri Dergisi, cilt.23, ss.78-89,

De Bei, R., Cozzolino, D., Sullivan, W., Cynkar, W., Fuentes, S., Dambergs, R., Pech, J. and Tyerman, S., 2011. Non-destructive measurement of grapevine water potential using near infrared spectroscopy. Australian Journal of Grape and Wine Research, 17(1), 62–71, doi: 10.1111/j.1755-0238.2010.00117.x

Deloire, A. and Carbonneau, A., Wang, Z. and Ojeda, H., 2004. Vine and water, a short review. Journal International des Sciences de la Vigne et du Vin, 38(1), 1-13.

Demirel K., Çamoğlu G., Genç L., Kizil Ü., 2014. The Variation of Plant Stress Indicators and Some Traits Under Different Irrigation and Nitrogen Levels In The Rocket. Fresenius Environmental Bulletin, vol.23, pp.1238-1248.

Demirel K., Çamoğlu G., Akçal A. (2018). Effect of Water Stress on Four Varieties of Gladiolus. Fresenius Environmental Bulletin, vol.27, no.12A/2018, pp.9300-9307.

Durgut, M.R. and Arın, S., 2005. Level and Problems of Trakya Region Vineyard Mechanization, Journal of Tekirdag Agricultural Faculty, 2(3), 287-297

Eamus, D. and Shanahan, S.T., 2002. A rate equation model of stomatal responses to vapour pressure deficit and drought. BMC Ecology. 2(8), 1-14, doi: 10.1186/1472-6785-2-8

Eitel, J.U.H., Gessler, P.E., Smith, A.M.S. and Robberecht, R., 2006. Suitability of existing and novel spectral indices to remotely detect water stress in Populus spp.. Forest Ecology and Management, 229(1-3), 170–182, http://dx.doi.org/10.1016/j.foreco.2006.03.027

Ferrini, F., Mattii, G.B. and Nicese, F.P., 1995. Effect of temperature on key physiological responses of grapevine leaf. American Journal of Enology and Viticulture, 46(3): 375-379.

Filella, I. and Penuelas, J., 1994. The red edge position and shape as indicators of plant chlorophyll content, biomass and hydric status. International Journal of Remote Sensing, 15(7), doi: 10.1080/01431169408954177

Fitzgerald, G.J., Rodriguez, D., Christensen, L.K., Belford, R., Sadras, V.O. and Clarke, T. R., 2006. Spectral and thermal sensing for nitrogen and water status in rainfed and irrigated wheat environments. Precision Agriculture, 7(4), 233-248, doi:10.1007/s11119-006-9011-z

Gao, B., 1996. NDWI a normalized difference water index for remote sensing of vegetation liquid water from space. Remote Sensing of Environment, 58(3), 257–266, http://dx.doi.org/10.1016/S0034-4257(96)00067-3

Govender, M., Dye, P., Weiersbye, I., Witkowski, E. and Ahmed, F., 2009. Review of commonly used remote sensing and ground-based technologies to measure plant water stress. Water SA, 35(5), 741-752, http://dx.doi.org/10.4314/wsa.v35i5.49201

Greenspan, M. D., Schultz, H. R. and Matthews, M. A., 1996. Field evaluation of water transport in grape berries during water deficits. Physiologia Plantarum, 97(1), 55–62, doi: 10.1111/j.1399-3054.1996.tb00478.x

Greer, D.H. and Weedon, M.M., 2012. Interactions between light and growing season temperatures on, growth and development and gas exchange of Semillon (Vitis vinifera L.) vines grown in an irrigated vineyard. Plant Physiology and Biochemistry, 54, 59-69. http://dx.doi.org/10.1016/j.plaphy.2012.02.010

Gürsoy, Ö. and Atun, R., 2018. Comparison of Spectral Classification Methods in Water Quality. Cumhuriyet Science Journal, 39-2(2018) 543-549, http://dx.doi.org/10.17776/csj.422897.

Gürsoy, Ö. and Atun, R., 2019. Using Remote Sensing in Detecting Sugar Beet Fields Treated with Different Doses of Phosphorus. Fresenius Environmental Bulletin, 28(2A), 1247-1253.

Gutierrez, M., Reynolds, M.P., and Klatt, A.R., 2010. Association of water spectral indices with plant and soil water relations in contrasting wheat genotypes. Journal of Experimental Botany, 61(12), 3291–3303, doi: 10.1093/jxb/erq156

Hunt, E.R. and Rock, B.N., 1989. Detection of changes in leaf water content using near- and middle infrared reflectances. Remote Sensing of Environment, 30(1), 43-54, http://dx.doi.org/10.1016/0034-4257(89)90046-1

İnce C., Özelkan E., Kaya Ş., 2014. Assessment of Thyme Reduction Using Multitemporal Satellite Data and In-Situ Spectroradiometric Measurement: Altioluk Plateau. Kocaeli-Turkey", FRESENIUS ENVIRONMENTAL BULLETIN, vol.23, pp.3007-3012.

Jayaraman, V. and Srivastava, S.K., 2002. The invariance of red-edge inflection wavelengths derived from ground based spectro-radiometer and space-borne IRS-P3: MOS-B data. International Journal of Remote Sensing, 23(14), 2741-2765, DOI:10.1080/014311602760128125

Kakani, V.G., Reddy, K.R. and Zhao, D., 2007 Deriving a simple spectral reflectance ratio to determine cotton leaf water potential. Journal of New Seeds, 8(3), 11-27, doi:10.1300/J153v08n03_02

Kennedy, J.A., Matthews, M.A., and Waterhouse A.L., 2002. Effect of maturity and vine water status on grape skin and wine flavonoids. American Journal of Enology and Viticulture, 53(4), 268-274.

Kokaly, R.F. and Clark, R.N., 1999. Spectroscopic determination of leaf biochemistry using band-depth analysis of absorption features and stepwise multiple linear regression. Remote Sensing of Environment, 67(3), 267-287, http://dx.doi.org/10.1016/S0034-4257(98)00084-4

Kokaly, R.F., 2001. Investigating a physical basis for spectroscopic estimates of leaf nitrogen concentration. Remote Sensing of Environment, 75(2), 153-161, http://dx.doi.org/10.1016/S0034-4257(00)00163-2

Lambers, H.F., Chapin, F.S. and Pons, T.L., 2008. Plant physiological ecology. 2nd Edition. Springer Sciences Business Media, LLC, doi: 10.1007/978-0-387-78341-3

Liu, L., Zhao, J. and Guan, L., 2013. Tracking photosynthetic injury of Paraquat-treated crop using chlorophyll fluorescence from hyperspectral data. European Journal Of Remote Sensing, 46, 459-473, doi: 10.5721/EuJRS20134627

Mohan, B.K., 2008. Hyperspectral Image Processing. ISRS Pre-Symposium Tutorial on "Hyperspectral Data Analysis and Applicaitons", December 16-17, 2008, SAC, Ahmedabad.

Mutanga, O. and Skidmore, A.K., 2003. Continuum-removed absorption features estimate tropical savanna grass quality in situ. 3rd EARSEL Workshop on Imaging Spectroscopy, Herrsching, 13-16 May 2003, 542-558. http://www.itc.nl/library/papers_2003/peer_ref_conf/mutanga.pdf

Naor, A., Bravado, B. and Gelobter, J., 1994. Gas exchange and water relations in field- grown 'Sauvignon blanc' grapevines. American Journal of Enology and Viticulture, 45(4), 423-428.

Ozelkan E., Karaman M., Candar S., Coskun Z., Ormeci C., 2015. Investigation of grapevine photosynthesis using hyperspectral techniques and development of hyperspectral band ratio indices sensitive to photosynthesis. Journal of Environmental Biology, vol.36, pp.91-100.

Ozelkan, E., Chen, G., Ustundag, B.B., 2016. Multiscale object-based drought monitoring and comparison in rainfed and irrigated agriculture from Landsat 8 OLI imagery. International Journal of Applied Earth Observation and Geoinformation, 44: 159-170. https://doi.org/10.1016/j.jag.2015.08.003

Peñuelas, J., Filella, I., Biel, C., Serrano, L. and Savé, R., 1993. The Reflectance at the 950–970 nm region as an indicator of plant water status. International Journal of Remote Sensing, 14(10), doi:10.1080/01431169308954010

Rodríguez-Pérez J.R., Riaño D., Carlisle E., Ustin S., and Smart D.R., 2007. Evaluation of hyperspectral reflectance indexes to detect grapevine water status in vineyards. American Journal of Enology and Viticulture, 58(3), 302–317.

Ritchie, G.A., Hinckley, T.M., 1975. The pressure chamber as an instrument for ecological research. Advances in Ecological Research, 9, 165–254.

Scholander, P.F., Hammel, H.T., Bradstreet, E.A. and Hemmingsen, E.A., 1965. Sap pressure in vascular plants. Science, 148(3668), 339-346, doi:10.1126/science.148.3668.339

ÇOMÜ Zir. Fak. Derg. (COMU J. Agric. Fac.)
2020: 8 (2): 475–489
ISSN: 2147–8384 / e-ISSN: 2564–6826
doi: 10.33202/comuagri.754784

Schultz, H.R. and M.A. Matthews., 1993. Growth, osmotic adjustment, and cell-wall mechanics of expanding grape leaves during water deficits. Crop Science, 33(2), 287-294, doi:10.2135/cropsci1993.0011183X003300020015x

Sims, D.A. and Gamon, J.A., 2002. - Relationships between leaf pigment content and spectral reflectance across a wide range of species, leaf structures and developmental stages. Remote Sensing of Environment, 81(2-3), 337– 354, http://dx.doi.org/10.1016/S0034-4257(02)00010-X

Sims, D.A. and Gamon, J.A., 2003. Estimation of vegetation water content and photosynthetic tissue area from spectral reflectance: a comparison of indices based on liquid water and chlorophyll absorption features. Remote Sensing of Environment, 84(4), 526–537, http://dx.doi.org/10.1016/S0034-4257(02)00151-7

Schmidt, K.S. and Skidmore, A.K., 2003. Spectral discrimination of vegetation types in a coastal wetland. Remote Sensing of Environment, 85(1), 92 – 108, http://dx.doi.org/10.1016/S0034-4257(02)00196-7

Sensoy, S., Demircan, M., Ulupinar, Y. and Balta, Z., 2008. Climate of Turkey. http://www.mgm.gov.tr/FILES/iklim/turkiye_iklimi.pdf

Smith, R. and Prichard, T., 2003. Using a Pressure Chamber in Winegrapes. UC Cooperative Extension, http://cesonoma.ucdavis.edu/files/27409.pdf

Stimson, H.C., Breshears, D.D., Ustin, S.L. and Kefauver, C., 2005. Spectral sensing of foliar water conditions in two co-occur- ring conifer species: Pinus edulis and Juniperus monosperma. Remote Sensing of Environment, 96(1), 108-118, http://dx.doi.org/10.1016/j.rse.2004.12.007

Tucker, C.J., 1980. Remote sensing of leaf water content in the near infrared. Remote Sensing of Environment, 10(1), 23-32, http://dx.doi.org/10.1016/0034-4257(80)90096-6

Turner, N.C., 1981. Techniques and experimental approaches for the measurement of plant water status. Plant and Soil, 58(1-3), 339-366, doi:10.1007/BF02180062

Turner, N.C., 1988. Measurement of plant water status by the pres- sure chamber technique. Irrigation Science, 9(4), 289-308, doi: 10.1007/BF00296704

Turkish State Meteorological Service (TSMS), 2013. Ozone and UV, http://www.mgm.gov.tr/arastirma/ozon-ve-uv.aspx?s=uv

Uzun, I., 2004. Viticulture Handbook. Hasad Publications, 1st edition.

Williams, L.E. and Araujo, F.J., 2002. Correlations among Predawn Leaf, Midday Leaf, and Midday Stem Water Potential and their Correlations with other Measures of Soil and Plant Water Status in Vitis vinifera. Journal of American Society for Horticulture Science, 127(3), 448-454.

Zarco-Tejada, P.J., Miller, J.R., Mohammed, G.H. and Noland, T.L., 2000. Chlorophyll fluorescence effects on vegetation appar- ent reflectance. I. Leaf-level measurements and model simulation. Remote Sensing of Environment, 74(3), 582-595, http://dx.doi.org/10.1016/S0034-4257(00)00148-6.